AN INVESTIGATION OF SPUDCAN PERFORMANCE IN A MULTI-LAYERED SOIL PROFILE

L. Sharp
J. Morton
J. Osborne

1 ABSTRACT

Accurate prediction of spudcan performance is crucial for the safe use of offshore jack-up platforms. Despite significant research over the last 50 years, accurately predicting spudcan installation performance in multi-layered soils remains a challenge. Unexpected leg penetration and punch-through failures still persist, which can have severe cost implications and endanger lives. This paper investigates spudcan penetration behaviour at 11 offshore wind turbine locations, in sand-clay soil profiles, with a high risk of punch-through failures. Load penetration analyses are compared to the recorded jack-up performance from high quality continuous jacking data and suggestions are made on how the predictive methods could be improved for future jack-up operations. The formation and evolution of a trapped soil plug beneath the spudcan is also discussed. The research finds industry-recommended failure models underpredict bearing capacity and should consider the formation of trapped soil plugs beneath the spudcans in layered soil conditions. An established feedback loop between the jack-up and predictors during installation is also key to increasing prediction accuracy particularly where cone penetrometer test data spread can provide a high degree of soil strength uncertainty.

2 KEY WORDS

Spudcan, punch-through, soil plug, jack-up.

3 INTRODUCTION

Mobile Jack-Up (JU) platforms are routinely used in offshore industries for oil and gas drilling, and windfarm construction. Oil and gas JU's are predominantly of the 3-leg design whereas the independent legged self-elevating construction vessels (JU's) used in the Offshore Renewables (ORE) Industry typically have 4 legs, with 6 units in the fleet having 6 legs. Bearing pads or "spudcans" are fitted to the base of the legs that transfer the load from the platform to the ground. Spudcans vary in shape and size but typically are shallow conical-shaped foundations with a sharp protruding spigot from the base. Recent research focuses on the behaviour of spudcans during penetration (e.g., [1/2/3/4]), yet incorrect predictions still persist, particularly in layered soil profiles. The primary risk associated with spudcans in multi-layered soils is punch-through failure, which is the predominate cause of JU accidents [5]. Punch-through occurs where stronger soils overlie weaker material. A peak bearing resistance (Q_{peak}) is initially achieved in the stronger layer, followed by a reduction in the bearing capacity as the footing pushes through the layer of the harder soil into the underlying softer layer. A leg suffering punch-through penetrates the ground without any additional loading at a rate which exceeds the leg jacking rate, until a depth where bearing capacity increases. This paper reports on the reliability of load penetration predictions for both Q_{peak} and deep bearing capacity at 11 turbine locations. Published Load Penetration Analyses (LPA's) methods are assessed, three of which utilise approaches outlined in ISO/ SNAME [6/7], one considers alternative failure models, namely Hu *et al*.'s (2014) stress dependant failure model to predict Q_{peak} and Craig and Chua's (1990) failure model to predict deep bearing capacities (below the sand-clay interface) [2/8].

4 SITE DATA

4.1 Ground conditions

The wind farm ground condition consists of 20 – 25 m of Quaternary sediments of both sand and clay overlying bedrock. The upper sand layer comprises two sub-layers; Unit Ia, a medium dense to dense sand, and, Unit Ib, a loose to medium dense sand. Below the sand, two over-consolidated clay formations are present (Unit II and III). Both are slightly sandy/ gravely and contain interbedded silt/sand beds. Several channel systems lie within the boundaries of these formations. Rockhead is located 20 – 25 m below seafloor and consists of slightly to

completely weathered sandstone Unit IVb, locally overlain by residual medium dense to dense sand Unit Iva (Figure 1 and 2).

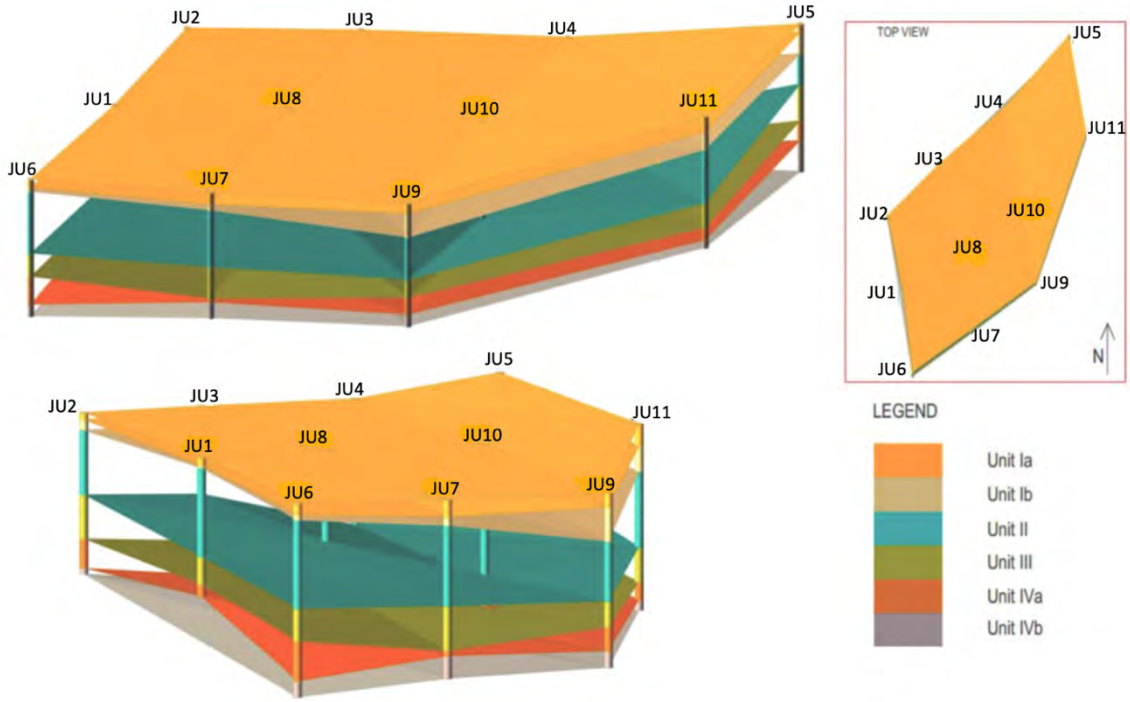

Figure 1. 3D ground model of the site (vertical exaggeration scale: 20 x H).

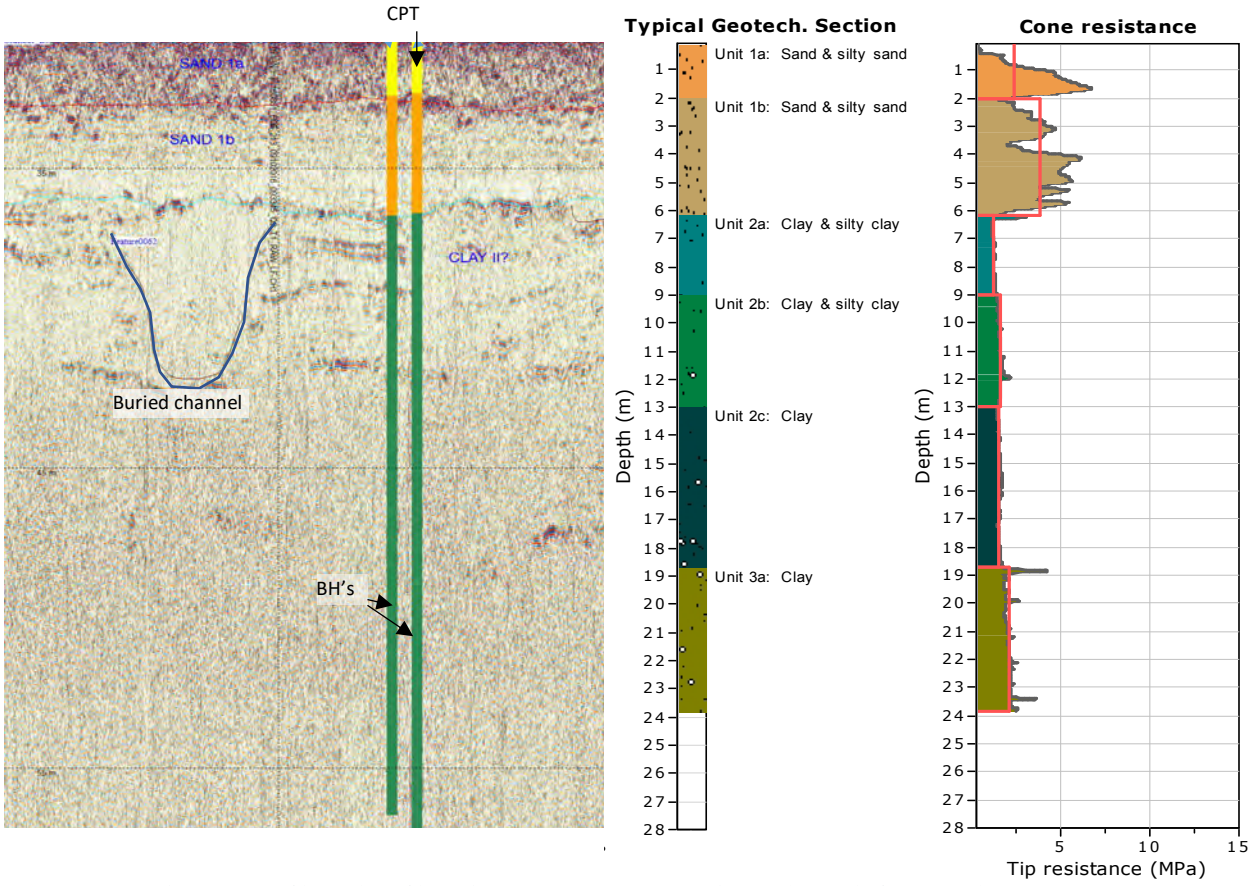

Figure 2. Typical seismic profile, soil profile and CPT cone resistance at the site (example from JU10).

4.2 Geohazards

The soil profile of sand over clay poses a risk of punch-through. The punch-through risk is most prevalent at locations where the sand is thickest. The possibility of scour induced punch-through has also been considered where the legs do not penetrate the sand during installation (i.e., where the legs remain '*hung up*').

Four levels of braided river deposits are distinguished within clay Units II and III across the site, with channels up to 60 m wide and 3 – 5 m deep. Channel infill deposits can be responsible for considerable lateral soil composition and strength variation, such that the soil strength beneath the spudcans could vary significantly to those at the nearest Cone Penetrometer Test (CPT)/ borehole location, creating a risk of unexpected leg penetration behaviour. Detailed interpretation of the data suggests the channel infill deposits across the site do not vary considerably in composition or strength and that Lower Bound (LB) and Upper Bound (UB) LPA's should account for any variation. At one location (JU5), however, a thick sand layer on the seabed (6 – 8 m) reduced seismic penetration which led to poor data received from the surveys and it was not possible to conclude whether any geohazards were present below Unit I.

4.3 JU

The turbine installation JU used at this Offshore Wind Farm (OWF) has six legs, each footed with a spudcan. The spudcans are conical in shape and dodecagonal in plan view, with an equivalent radius of c. 5.5 m and a full contact area of 95.4 m^2. Each leg (with footing) weighs 972 tons and the maximum predrive is 9650 tons/leg. The chosen design predrive footing reaction is 7600 tons/leg and the stillwater footing reaction is 5475 tons/leg. The distance from the spudcan base (full contact) to the spudcan tip is 0.739 m and the equivalent internal base angle is calculated at 8º (Figure 3).

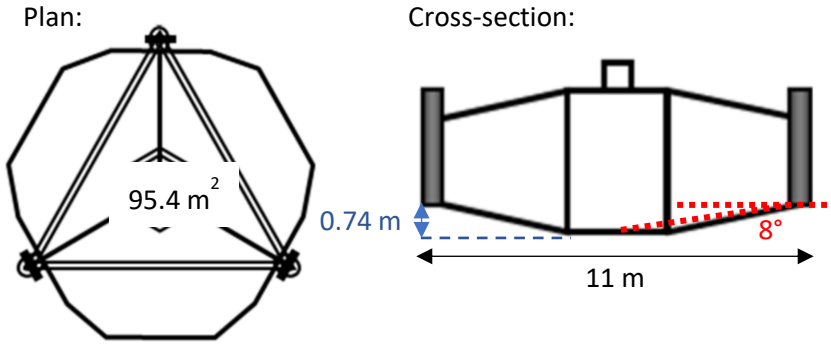

Figure 3. Spudcan geometry.

5 PREDICTIVE METHODS

JU leg penetration assessments are typically addressed by making predictions based on "upper estimate" and "lower estimate" soil strengths, derived from CPT data. Upper and lower bearing capacity estimates (the UB's and LB's) in turn produce prediction ranges for the design predrive footing reaction (7600 tons/leg). This section describes 4 predictive methods used for LPA's at this development. Methods 1 and 2 are the LPA's which were generated for the planned JU installations during windfarm construction. While Methods 3 and 4 have been used to test alternative predictive methods and develop a better understanding of Prediction Methodology 1. Note that limited information was provided as to how the Method 1 predictions were conducted.

Prediction Method 1: In general, predictive LPA's are conducted according to approach recommended by ISO. The fact that the analyst has applied this methodology is often the only statement accompanying their reports, without any information provided on how the methodology has been applied. For example, typically there is no information on the selection of the cone factors (N_{kt}'s) used to correlate the CPT cone tip resistance to the soil shear strength.

ISO recommend the application of Wished-In-Place (WIP) analyses for bearing capacity predictions in sand-clay soil profiles and this would appear to have been applied by the LPA analysts. For the punching shear 'WIP' failure model initially the bearing capacity is calculated based on the strength of the underlying (weak) clay with the addition of shearing resistance from a soil plug in the stronger crust (sand). The soil plug is then assumed to

disappear as the spudcan penetrates deeper through the strong crust (sand). At the boundary between the sand and clay bearing capacity is calculated using only the properties of the underlying clay (Figure 4).

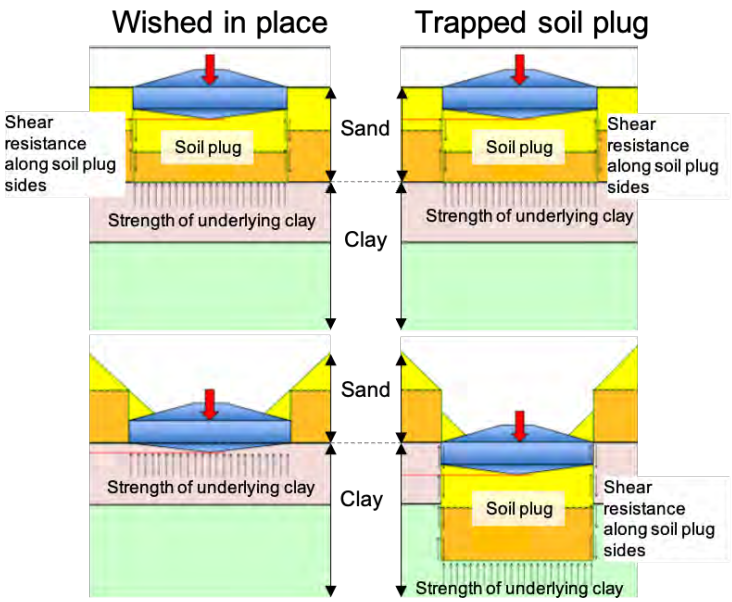

Figure 4. Schematic of a spudcan penetrating through sand over clay, showing the difference between 'wished-in-place' and 'trapped plug' analysis, edited from [9].

Prediction Method 2: The LPA analyst appears also to have followed the guidance provided by SNAME and ISO. The spudcan bearing capacity has been calculated based on Brinch Hansen's theory and an in-house program developed by the predictor from spudcan penetration prediction experience, which incorporates different failure mechanisms during the footing penetration in a multi-layered soil profile. In their analysis a soil plug has been considered to be present beneath the spudcan. Considering a trapped soil plug beneath the spudcan means calculated deep bearing capacity is higher than from punching shear (WIP) analysis as the soil plug acts as an extension to the spudcan. Thus, the shearing resistance around the plug increases the bearing capacity below the sand-clay interface (Figure 4). LB assessments have considered full backflow without any backflow for the UB condition. In addition to traditional LPA's methods, Finite Element Analysis (FEA) have also been applied to calculate Q_{peak} at 4 WTG locations (JU5, JU7, JU8, JU11). Traditional LPA's have been adjusted at locations where FEA indicates a different failure pattern to traditional LPA methods. Narrow range predictions were provided, using N_{kt} = 15 – 20 and broader range predictions where N_{kt} = 13 – 24 to consider scattered CPT data. In addition to this the predictions state uncertainty in deriving the N_{kt} factor for Unit III; caused by a large data spread and a large interval between lower and upper bound soil profiles.

Prediction Method 3: The Method has utilised Hu *et al.'s* (2014) stress dependant model to calculate Q_{peak} [2]. This failure model assumes an inverted truncated-cone shaped soil plug is pushed down beneath the spudcan. A shear surface develops inclined to the vertical at an angle corresponding to the dilation angle of the sand. The model also considers the stress level and dilatant response of the sand in Q_{peak} predictions (Figure 5). Deeper bearing capacity calculations (below the sand-clay interface) consider a soil plug the height of the top sand layer trapped beneath the spudcan. Craig and Chua's (1990) failure model has been used for LB and UB predictions unless Houlsby and Martin's (2003) model, adapted to consider a soil plug, provided a greater bearing capacity.

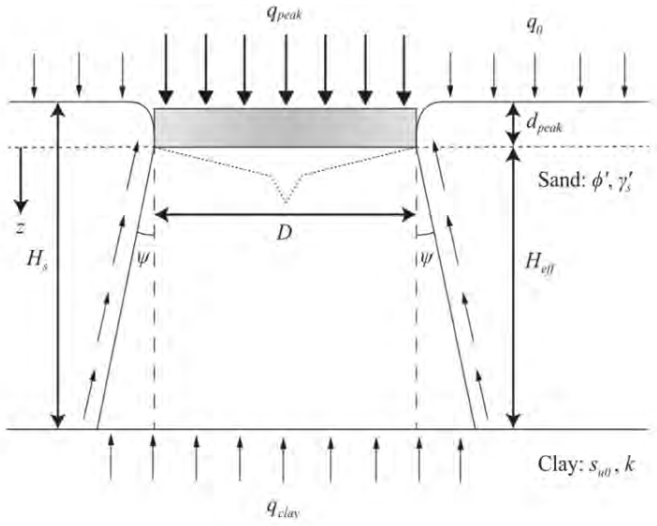

Figure 5. Schematic of Hu et al.'s (2014) stress dependent failure model [2]. H_s = Height of sand, H_{eff} = Effective height of sand, d_{peak} = depth of q_{peak}, Ψ = Dilation angle, D = Spudcan diameter.

Prediction method 4: This Method employed a simple WIP analysis as recommended in ISO, using Hanna and Meyerhof's (1980) failure model to calculate punch-through bearing capacity in the sand and Houlsby and Martin's (2003) model in the clay [10/11]. Full backflow has been considered in LB predictions without any soil backflow for the UB condition.

6 COMPARISON OF PREDICTIONS WITH ACHIEVED PENETRATIONS

6.1 Results overview

Final spudcan tip penetrations have been recorded for all legs at the 11 JU positions and final leg penetration ranges have been plotted alongside the predicted ranges for the 11 JU positions. Thickness of the top sand varied from 1 – 8.5 m across the site. The results have been divided into locations with > 3 m top sand and locations with < 3 m top sand (Figure 6). Typical spudcan penetrations ranged between 10 – 20 m, with little variability (< 2.5 m) between all 6 legs. Position JU5 provides an acception to this, where the final leg penetrations ranged from 2.5 – 21 m. One leg was deliberately left hung-up due to installation time pressures and penetration of the other five punched-through legs varied from 12 – 21 m depth (Figure 9(b), P. 9). The large range of final spudcan penetrations may have resulted from unmapped braided river deposits producing lateral strength heterogeneity (*as previously described*).

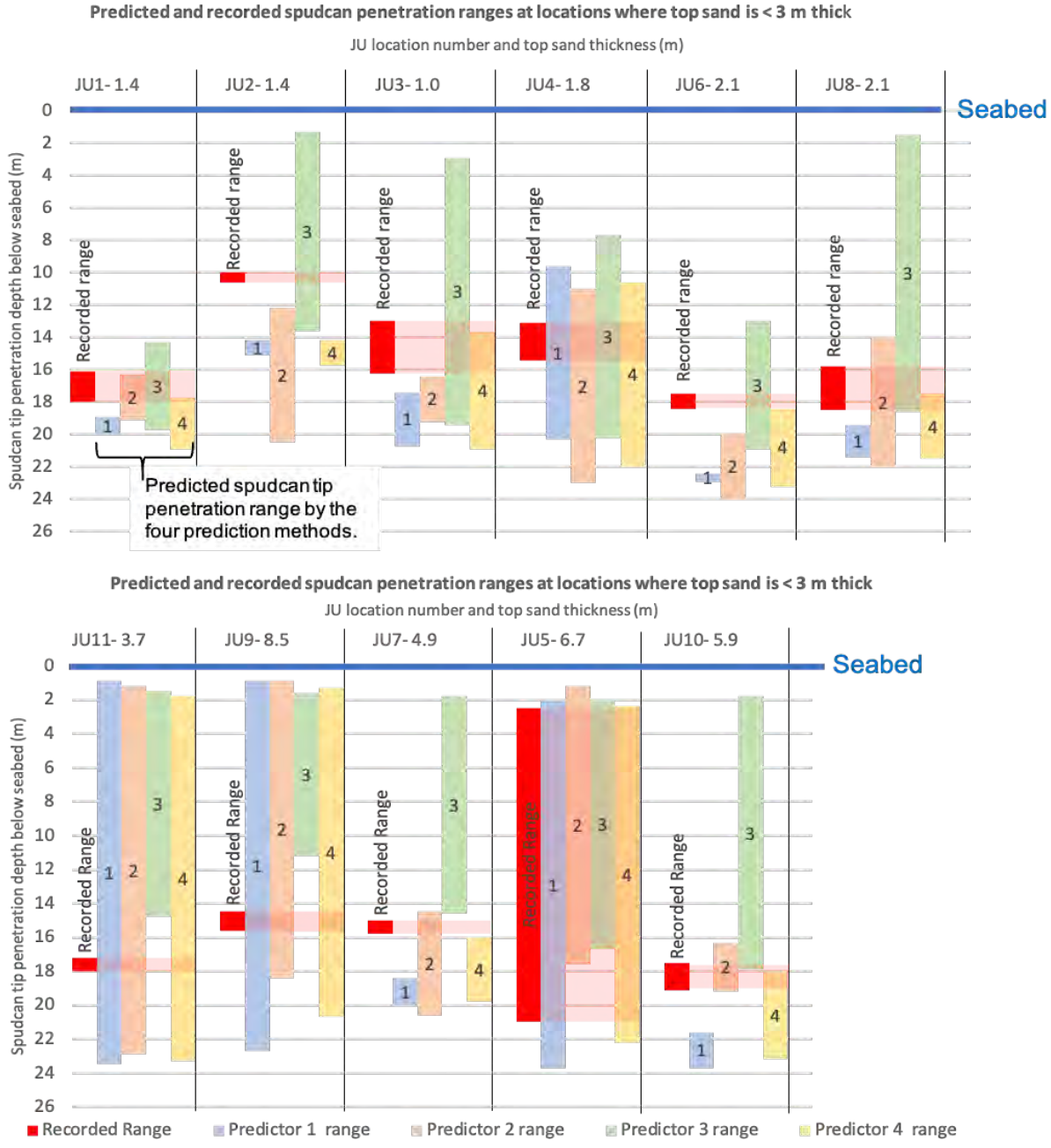

Figure 6. Predicted and recorded spudcan penetration ranges for the 11 JU positions. Location labels include the top sand height (m) at the position and results are categorised into positions with <3 m top sand (top) and >3 m top sand (bottom).

Although the spudcan penetration range plots (Figure 6) provide a good starting point to assess the reliability of predictions, results can be misleading at locations with a thicker top sand layer, where a possibility of both hung-up and punched-through legs resulted in large, predicted penetration ranges. For example, at locations JU9 and JU11 the spudcan penetration ranges in Figure 6 indicate good reliability for the Prediction Methods 1 and 4, which use WIP analyses, and final leg penetrations are correctly predicted. Bearing capacity depth graphs, however, show this is not the case and spudcan penetration has been overpredicted by both methods at both locations (final penetrations lie above UB predictions) (e.g., Figure 7). Reliability of predictions is thus reported from interpreting plots not just ranges.

Method 1's WIP analyses have provided narrow footing penetration prediction ranges which, overpredicted leg penetration at 7 out of the 11 JU locations and only 12 % of final leg penetrations lie within the lower and upper bounds. Prediction Method 4 utilised a similar failure model which provided slightly larger prediction ranges yet still overpredicted leg penetration at 7 locations and just 30 % of final leg penetrations lie within LB's and UB's.

Prediction Method 3 considered a trapped soil plug the height of the sand thickness below the spudcan, which increased the predicted bearing capacity and reduced the expected spudcan penetration compared to Methods 1 and 4. This model underpredicted leg penetration at 5 locations and correctly predicted 59 % of final leg penetrations. Also, Hu *et al.'s* (2014) failure model used here appears to have produced high Q_{peak} values across the site, resulting in large, predicted penetration ranges even when top sand is relatively thin (e.g., JU2, JU3 and JU8).

Method 2 underpredicted the bearing capacity at 3 locations and overpredicted it at 1 position. This bearing capacity failure model also considered a trapped soil plug and produced the most reliable predictions. Broad range predictions are correct for 89 % of final leg penetrations, which almost meets the 90 % benchmark outlined by InSafeJIP, a joint industry project aiming to improve safety of JU operations [12]. However, these predictions, left too much uncertainty as to the leg penetrations to be expected although the narrow range predictions were correct for 68 % of legs. The predictors did state spread of CPT data left uncertainty in the strength of the Unit III clay and requested feedback from the JU to confirm the soil strength during installation. Whilst this didn't happen it could have led to improved predictions at the time.

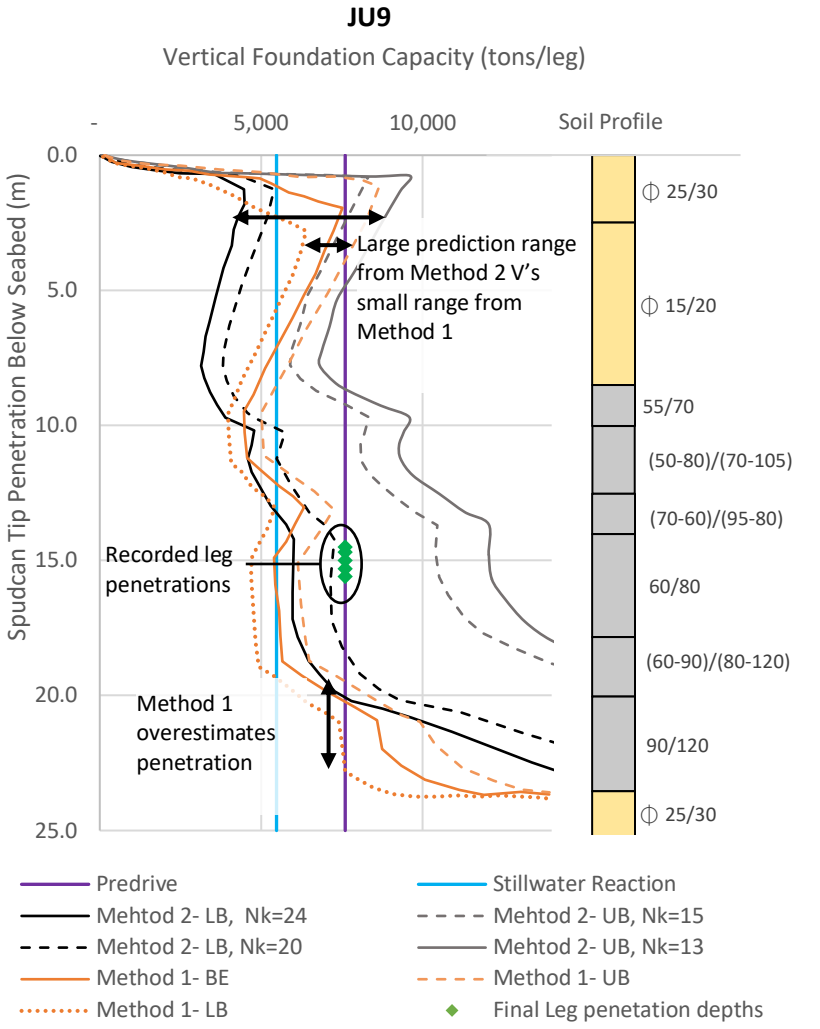

Figure 7. LPA's produced by Predictive Method 1 and 2 for JU9, the final leg penetrations and the soil profile are also plotted. Method 1's (WIP) analysis prediction range (0.9 – 23 m) covers final leg penetrations, however, deep bearing capacity is actually underestimated (final leg penetrations are above UB predictions). Also, a comparatively large prediction range is provided by Method 2.

6.2 Analyses of predictions from jacking logs

Jacking logs were recorded during unit installation which included loads at the jacks (measured with load cells in jack houses) and spudcan tip penetrations (measured with displacement transducers). These data provided an insight into the load required to cause further leg settlement and the soil bearing capacity throughout the depth of penetration achieved.

6.2.1 Peak bearing capacity

High quality jacking data in the shallow sediments (< 4 m depth) are available for 4 locations (JU4, JU5, JU7 and JU11). The load required to advance the spudcan through the stronger sand layer was taken as an estimate of Q_{peak}. For example, Figure 8 shows jacking data from the top 2.5 m of sediments at JU7, here Q_{peak} is consistent at approximately 7670 tons/leg. Also shown in Figure 8 are the Best Estimate (BE) predictions for Q_{peak} using the four predictive methods described in Section 5.

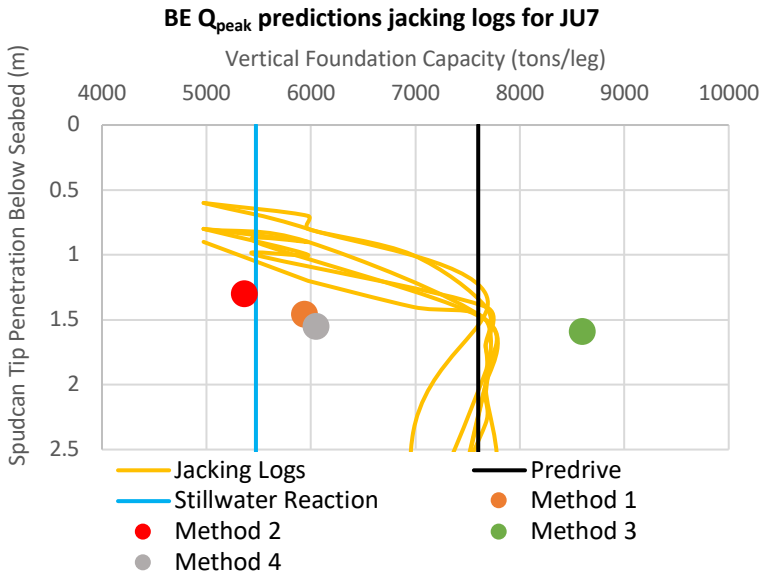

Figure 8. BE peak bearing capacity predictions and digitized jacking logs for JU7.

Table 1 shows the estimated and predicted $Q_{peak's}$ for JU4, JU5, JU7 and JU11. Predicton Methods 1 and 4 both utalised Hanna and Meyerhof's (1980) failure model for sand over clay to calculate Q_{peak}, values are thus very similar and only results from Prediction Method 1 are included in Table 1. Also, two Q_{peak} values are reported for Hu *et al.'s* (2014) failure model at each location. One is the value calulated by Predictive Method 3 and considers a conical shaped spudcan, the second is a recalculated value which considers a flat bottomed spudcan, reason for including the second adjusted value is discussed below.

Typically, higher Q_{peak} values were calculated from Hu *et al.'s* (2014) failure model compared to other failure models and BE's often slightly overpredict Q_{peak}. At JU5 Q_{peak} was significantly overpredicted and the recorded value was lower than the predicted range. The predictor expressed difficulty applying the failure model at this location due to a presence of multi-layered clay below the sand with varying strength, perhaps unrealistic resolving of the clay

Table 1. Comparison of Q_{peak} predictions to estimates from jacking data at JU4, JU5, JU7 and JU11. Cells are coloured yellow where the recorded Q_{peak} is outside predicted bounds.

JU4	**Q_{peak} from jacking data: 5070**		
Prediction method	**Q_{peak} LB**	**Q_{peak} UB**	**Q_{peak} BE**
1. Hanna and Meyerhof	3341	4979	4116
2. ISO & FEA	2403	5420	3461
3. Hu *et al.*	4856	7055	5955
Hu *et al.* (flat bottom D_F)	4431	5930	5180
JU5	**Q_{peak} from jacking data: 8200**		
Prediction method	**Q_{peak} LB**	**Q_{peak} UB**	**Q_{peak} BE**
1. Hanna and Meyerhof	7184	10429	8728
2. ISO & FEA	5284	12312	8200
3. Hu *et al.*	9719	14930	12003
Hu *et al.* (flat bottom D_F)	8339	11898	10119
JU7	**Q_{peak} from jacking data: 7670**		
Prediction method	**Q_{peak} LB**	**Q_{peak} UB**	**Q_{peak} BE**
1. Hanna and Meyerhof	4903	7000	5940
2. ISO & FEA	3291	7834	5363
3. Hu *et al.*	6442	9397	8593
Hu *et al.* (flat bottom D_F)	5830	8387	7109
JU11	**Q_{peak} from jacking data: 8000**		
Prediction method	**Q_{peak} LB**	**Q_{peak} UB**	**Q_{peak} BE**
1. Hanna and Meyerhof	5905	8648	7180
2. ISO & FEA	4721	9566	7144
3. Hu *et al.*	6262	10110	8187
Hu *et al.* (flat bottom D_F)	5748	8688	7218

layers may have caused this inaccuracy. The consistently slightly high estimates of Q_{peak} could be attributed by the Distribution Factor (D_F), which is defined as the ratio of the normal effective stress along the failure slip surface to the mean vertical effective stress. Soil distribution is a function of the ratio of Sand Height (Hs) to Footing Diameter (D) (Hs/D) and spudcan geometry. A steeper underside of a spudcan will invoke higher lateral stress and a higher distribution factor. This increases resistance along the slip surface. The D_F decreases as the Hs/D increases. The spudcans geometry considered by Hu *et al.* (2014) for the development of his method is different to that considered here. Here the JU was fitted with, flatter based spudcans which didn't have spigots. The equivalent base angle here is calculated to be 8° from the horizontal compared to 13° in the model development (Figure 3, P. 3). Therefore, less lateral stress and lateral distribution of soil is expected beneath this spudcan and a lower peak bearing capacity could be expected. Peak bearing capacities have been recalculated using D_F's intended for a flat-bottomed footing (from [1]), with the results also presented in Table 1. Typically, this adaption improved the predictions using the failure model and altered predictions are considered acceptable at all locations. The true D_F may be expected to lie between the two calculated D_F's. These results indicate a need for further research and development of D_F's to consider a wider range of spudcan geometries. Additionally, it must be noted Hu *et al.'s* failure model is developed for Hs/ D ratios 0.16 – 1, so that the model thus may not be suited to positions JU1, JU2 and JU3 where this ratio is < 0.16.

Hanna and Meyerhof's (1980) failure model (used by Prediction Methods 1 and 4) typically has provided low estimates for Q_{peak} (other than at JU5). Prediction Method 2 also used ISO/ SNAME methods to calculate Q_{peak}, this method too delivered low BE values for Q_{peak}, although their larger prediction ranges consistently cover the recorded Q_{peak}'s within LB's and UB's. Overall, it appears industry recommended methods slightly underestimated $Q_{peak.}$ This trend has also been observed by others [13].

At JU5 different result trends are observed and all predictive methods BE's overpredicted $Q_{peak,}$ excluding Method 4 which proved to provide reliable values (Table 1). At this location multiple clay layers of varying strength underlie the sand (annotated onto Figure 9(b), P. 9). All predictions other than Method 2 (which incorporated FEA) use failure models based solely on a two-layer system (sand over clay) meaning clay layers beneath the sand must be resolved to a singular layer to apply the failure models. Simplification of the ground failure to fit limiting equilibrium equations may have resulted in higher Q_{peak} values. Alternatively, Prediction Method 2 based their predictions at JU5 on FEA, which can incorporate more complex soil failures with interaction between the clay layers during failure. This appears to have aided the prediction of Q_{peak} at JU5.

6.2.2 Deep bearing capacity

BE LPA's (computed from the four methods) and jacking data are provided for two typical sand-over-clay ground conditions. Firstly, a thin sand layer located at JU6 is shown in Figure 9(a). In this location the sand is less than 2 m thick. Secondly, a larger sand layer is shown in Figure 9(b) corresponding to JU5. This area is characterised with sand, approximately 6 m thick. The range of sand over clay thickness highlighted here is not uncommon at OWF developments. Below the sand layers, are clay layers of various thickness and strength (soil profiles are annotated onto Figures 9(a & b). Spudcan deep bearing capacity is linked to the undrained shear strength of the underlain clay [6]. The selections of strength parameters for clay is challenging and is typically based on CPT analysis. In this study, predictors appear to regularly underestimate clay strength (e.g., Figure 9(a)), partially due to the wide range of cone bearing capacity factors [14]. An established loop between the JU and predictors during the installation program could have eliminated these soil strength uncertainties from experience and significantly improved prediction reliability throughout the installation program.

Frequently in layered ground conditions the observed JU leg penetration behaviour suggests that trapped soil plugs are formed. Method 1 and 4's LPA's apply WIP analysis, and both analyses overestimated the spudcan penetration depth. This is mainly due to the omission of the bearing capacity provided from a soil plug in the clay (described in Section 5). As bearing capacity provided from a soil plug in the clay is not included the WIP method is unrepresentative of the actual ground failure mode and overestimated penetration depth.

Prediction Method 3 incorporates Craig and Chua's (1990) algorithm which considers a trapped soil plug failure model, although is observed to underestimate the increase of bearing capacity with depth. The model also overpredicts bearing capacity immediately below the sand-clay interface where the top sand layer is thin (< 2.5 m thick). Unlike ISO recommended clay bearing capacity calculations, Craig and Chua's (1990) method does not include a depth factor in the equation, which is likely the cause of these issues. Where the sand is < 2.5 m thick, the use of WIP analysis could be considered more appropriate than Craig and Chua's (1990) method. WIP analysis, however, overestimates final leg penetrations even when the sand is < 2 m thick. Either additional friction from a small soil plug is increasing bearing capacity or the soil strength is underestimated. At location JU2 soil strength has been underestimated and bearing capacity is underpredicted even when a soil plug is considered.

Prediction Method 2 also considers a trapped soil plug in the predictions (although the specifics of the soil plug's are not specified by the predictor). Their deep bearing capacity predictions are typically best where top sand is thicker and often underpredict deep bearing capacity when sand is < c.2 m thick. Alternatively, the assumption that the soil plug develops and remains the height of the sand layer by Craig and Chua's method (Prediction Method 3) leads to underestimating final penetration depths at locations with thicker sand layers.

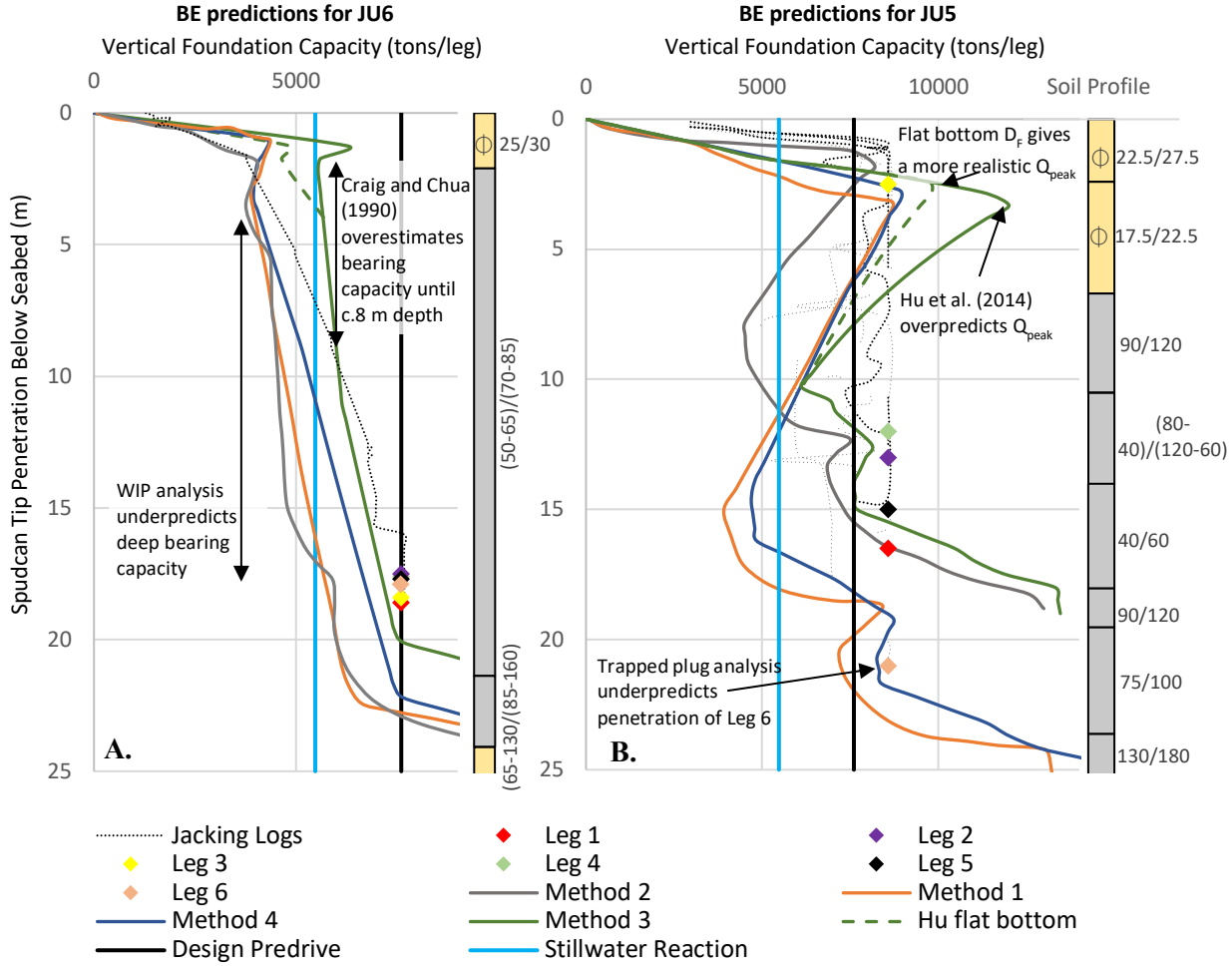

Figure 9. Example LPA's from the site for JU6 (a) and JU5 (b), showing the BE predictions provided by the 4 predictors.

6.3 Evolution of the soil plug

Comparison of jacking data and predictions at locations with a sand layer > 3 m thick (JU10, JU7, JU11, JU5 and JU9) helps develop an understanding of soil plug evolution at the OWF. The formation and evolution of a soil plug is primarily controlled by the soil profile and spudcan geometry. As outlined in Section 6.2 WIP analyses typically overpredicts deep spudcan penetrations and trapped plug analyses typically underpredicts deep spudcan penetrations when a soil plug with a height equal to the top sand thickness is considered. This indicates either a

shorter soil plug is forming, and/ or the soil plug is evolving (eroding) during continued penetration. In reality both these factors are likely to be affecting the deep bearing capacity.

LPA's for locations with Hs > 3 m, produced from Craig and Chua's (1990) failure model have been used to explore the soil plug evolution. Locations JU10, JU7 and JU11 have similar soil profiles of sand (4.9 – 8.5 m thick) over clay with gradually increasing strength to 20 – 24 m beneath the seafloor. Below this clay, a much stronger clay layer creates a rapid increase in bearing capacity (soil profiles are annotated onto Figure 10(a – c). The difference in depth between final leg penetrations and the increase in bearing capacity indicate on average c. 71 – 84 % of the soil plug has remained intact at these locations (Table 2). Final leg penetrations suggest the minimum retained thickness of the soil plug from these locations is c. 62 % at JU11. Reproduced bearing capacity curves considering 40 % erosion of the soil plug in LB estimates correctly predict all final leg penetrations (Figure 10). Thus, considering a trapped soil plug of height 0.6Hs in LB predictions appears appropriate at locations with sand over a thick continuous clay layer.

Table 2. Average height of soil plug remaining at final leg penetration depth.

Location	Hs (m)	Av. thickness of soil plug at final penetration (m)	Difference between Hs & soil plug thickness (m)	Av. final leg penetration depth (m)	Av. remaining soil plug (%)
JU11	8.5	6.0	2.5	17.4	71
JU10	5.9	4.6	1.3	18.3	78
JU7	4.9	4.1	0.8	15.4	84

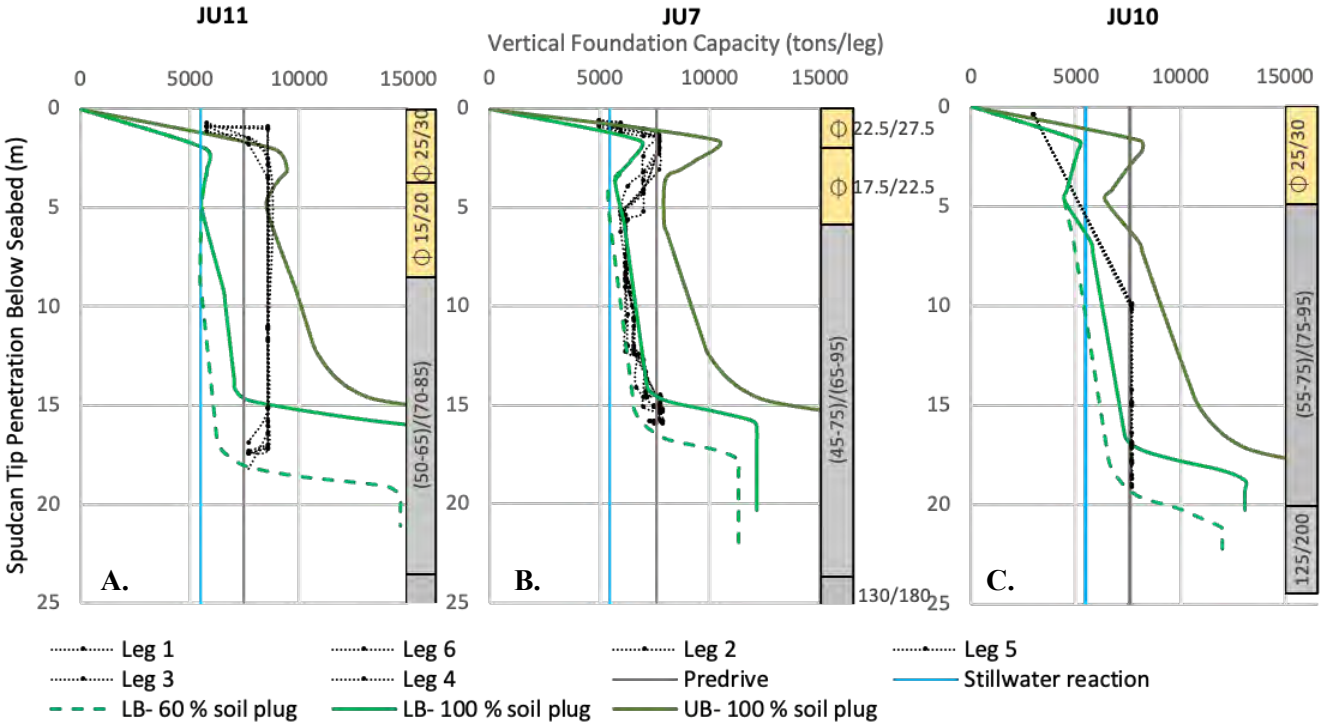

Figure 10. LPA's produced from Craig and Chua's failure model at JU11 (a), JU10 (b) and JU7 (c), adjusted to consider 40 % erosion of the soil plug in LB prediction.

JU5 and JU9 have more complex soil profiles and final leg penetrations suggest at both these locations the soil plug has eroded more than 40 %. For both JU5 and JU9 below the top sand, the soil profile consists of multiple clay layers (1.5 – 3.8 m thick) with varying strength, a stronger clay layer is interbedded between two weaker units at (12.5 m depth at JU9 and 18 m depth at JU5). Details of locations soil profiles are annotated onto Figures 9(b), P. 9 and Figure 7, P. 6). Penetration of the legs through these comparatively stronger layers here (at 12.5 m and

18 m depth) appear to have increased the soil plug erosion and led to subsequent deeper leg penetration. At JU5 and JU9 around 50 % soil plug erosion must be considered to correctly predict the deepest leg penetrations (52 % at JU5 and 51% at JU9), indicating where multiple clay layers are encountered more soil plug erosion should be anticipated.

7 CONCLUSIONS

- The spudcan penetration behaviour at the windfarm suggests a soil plug initially became trapped beneath the spudcan during installation at all JU locations. A trapped soil plug should thus be considered in future spudcan penetration predictions at this windfarm.
- ISO recommended WIP analyses doesn't accurately model the ground failure here as omission of additional bearing capacity provided from a trapped soil plug leads to overestimates of final penetration depths. This is a common issue in sand-clay soil profiles and as widely reported (e.g., [15/16/2/9]).
- ISO recommended methods also provided conservative estimates for Q_{peak} and Hu *et al.'s* (2014) stress-dependent failure model proved a good alternative for Q_{peak} calculations in this instance although further development of the D_F is necessary to calibrate the model for an appropriate range of spudcan geometries.
- The evolution of the soil plug with continued spudcan penetration varied across the site and appears to have been largely controlled by strength contrasts between the clay layers, where interaction of the soil plug with a relatively stiff clay was associated with increased erosion of the soil plug. Leg penetration depths suggest at all locations a soil plug with a thickness > 45 % of Hs remained beneath the spudcan at final leg penetration depths. Further research is required to develop a method to predict soil plug evolution beneath a spudcan with deep penetration.
- Communication between the JU and predictors during installation should be used to refine predictions throughout the program and is vital to increase the reliability of narrow range predictions where spread in CPT data has left uncertainty in the soil strength.
- High quality jacking data is crucial to improving spudcan penetration predictions. The requirement for detailed jacking logs is not well understood and should be promoted to enable back analysis of LPA's and improvements to be made for future predictions.

8 REFERENCES

[1] Lee, K. K., Randolph, M. F., and Cassidy, M. J. 2013. Bearing capacity on sand overlying clay soils: A simplified conceptual model, Geotechnique, **63(15),** 1285-1297.

[2] Hu, P., Stanier, S. A., Cassidy, M. J. and Wang D. 2014. Predicting peak resistance of spudcan penetrating sand overlying clay, Journal of Geotechnical and Geoenviromental Engineering (ASCE), **140(2)**, 04013009(1-12).

[3] Hossain, M. 2014. Experimental investigation of spudcan penetration in multi-layer clays with interbedded sand layers, Geotechnique, **64(4),** 258-277.

[4] Gao. W. 2017. Large penetration of spudcan foundation in multi-layered clay- numerical study, PHD Thesis, The University of Western Australia, School of Civil Environmental and Mining, Centre for Offshore Foundation Systems.

[5] Dier, A., Abolfathi, S., Carroll, B. and Britain, G. 2004. Guidelines for jack-up rigs with particular reference to foundation integrity, MSL Engineering Limited, research report 289, HSE Books.

[6] ISO International Organization for Standardization. 2012. Petroleum and Natural Gas Industries – Site Specific Assessment of Mobile Offshore Units – Part 1: Jack-ups, International Standard ISO 19905-1:2016.

[7] SNAME Guidelines for site specific assessment of mobile jackup units. 2002. The Society of Naval Architects & Marine Engineers, Jersey, City, NJ, USA, Technical and Research Bulletin, 5-5A.

[8] Craig, W. H. and Chua, K. 1990. Deep penetration of spudcan foundation on sand and clay, Geotechnique, **40(4)**, 541-556.

[9] Overy, R. F. and Hunt R. J. 2019. Spudcan penetration assessment with a trapped soil plug, Proc. of the 17th International Conference: The Jack-Up Platform, University of London, England.

[10] Hanna, A. M. and Meyerhof, G. G. 1980. Design charts for ultimate bearing capacity of foundations on sand overlying soft clay, Canadian Geotechnical Journal, **17(2),** 300-303.

[11] Houlsby, G. T. and Martin, C. T. 2003. Undrained bearing capacity factors for conical footings on clay, Geotechnique, **53(5),** 513-520.
[12] Osborne, J. J., Nelson, C. and Hunt, R. 2008. An introduction to InSafeJIP, Proc. of the 2nd Jack-up Asia Conference and Exhibition, PetroMin, Singapore.
[13] Lee, k. k. 2009. New Simplified Conceptual Model for Spudcan Foundations on Sand Overlying Clay Soils, Proc. of the OTC 20012.
[14] Lunne, T., Robertson, P. K. and Powell, J. J. M. 1997. Cone Penetration Testing in Geotechnical Engineering, Blackie Academic and Professional, London.
[15] Teh, K. L., Leung, C. F., Chow, Y. K. and Handidjaja, P. 2009. Prediction of punch-through for spudcan penetration in sand overlying clay, Proc. of the 41st Offshore Technology Conference, OTC20060, Houston.
[16] Lee, K. K., Cassidy, M. J., and Randolph, M. F. 2013. Bearing capacity on sand overlying clay soils: Experimental and finite element investigation of potential punch-through failure, Geotechnique, **63(15),** 1271-1284.